Supplementary Figure 1: Derivation of Cohort

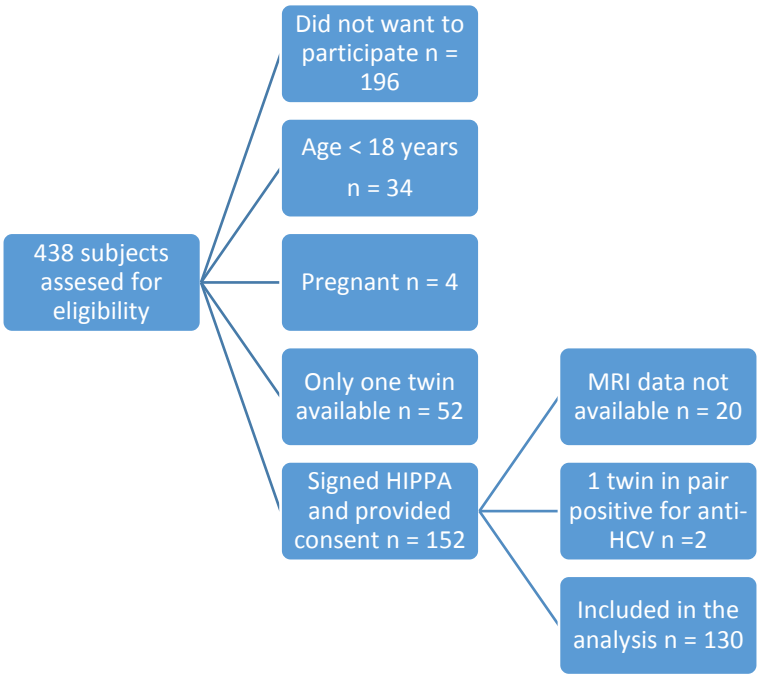

Supplementary Figure 1: 438 subjects were assessed for eligibility, and 152 patients signed HIPPA and provided consent. Of these 152 subjects, 20 (10 twin pairs) were excluded because MRI data was not available, and 2 (1 twin pair) was excluded because one of the twins tested positive for anti-HCV. A total of 130 subjects was included in the final analysis.

Questions used to determine zygosity:

1. Were you and your twin “as alike as two peas in a pod”?

   As alike as two peas in a pod

   Usual sibling similarity

   Quite different

2. Were you and your twin mixed up as children?

   Yes, very often

   Now and then

   Never

3. In that case, by whom were you mixed up?

   Parents

   Teachers

   Others

   Nobody (1)

Clinical Research Assessment:

All participants underwent clinical research assessments at the UCSD NAFLD Research Center. A trained investigator performed physical and anthropometric exams, which included vital signs, height, and weight. Blood pressure was measured using an automatic blood pressure cuff after the patient had remained seating for five minutes. Weight was measured using an electronic scale from seca (Hamburg, Germany). Body mass index (BMI) was defined as body weight in kilograms divided by height in meters squared. Medical history, including the use of steatogenic drugs, was obtained from all participants. Alcohol use history was ascertained using the Alcohol Use Disorders Identification Test (AUDIT) and

Skinner lifetime drinking history questionnaires. The following fasting biochemical profiles were obtained from all participants: glucose, insulin, hemoglobin A1c, homeostatic model assessment of insulin resistance (HOMA-IR), aspartate aminotransferase (AST), alanine aminotransferase (ALT), alkaline phosphatase (Alk P), total bilirubin, direct bilirubin, albumin, gamma glutamyltransferase (GGT), total cholesterol, high-density lipoprotein (HDL), low-density lipoprotein (LDL), triglycerides, white blood cell count, hemoglobin, hematocrit, platelet count, international normalized ratio (INR), and ferritin. LDL cholesterol was calculated using the formula (total cholesterol – HDL) – (triglycerides/5). Participants fasted for a minimum of eight hours overnight before biochemical profiles were collected.

Inter-reader reproducibility of MRI-PDFF:

MRI-PDFF has high inter-reader reproducibility, with whole-liver ICC of 0.965 (95% CI: 0.952, 0.975) and individual-segment ICCs ranging from 0.933 (95% CI: 0.889, 0.958) for segment 1 to 0.983 (95% CI: 0.973-0.987) for segment 8.(2)

Magnetic Resonance Elastography:

MRE was performed using previously published methods(3-8) using software and hardware available commercially from Resoundant Inc., Rochester, MN. Briefly, an acoustic active driver placed outside of the MRI room delivers continuous vibrations at 60 Hz to an acoustic passive driver attached with an elastic band to the body wall anterior to the liver. During the transmission of the vibrations, a 2D gradient-recalled-echo MRE pulse sequence is performed, leading to the acquisition of four non-contiguous axial slices, 10-mm thick with 10-mm interslice gaps, that were acquired in a 16-second breathhold through the widest transverse section of the liver. The following acquisition parameters were used: repetition time 50 ms, echo time 20.2 ms, flip angle 30 degrees, matrix 256 x 64, field of view

48 x 48 cm, one signal average, receiver bandwidth ± 33 kHz (confirm), and parallel imaging acceleration factor 2. The pulse sequence utilizes oscillating motion-sensitizing gradients which encode tissue motion into MR signal phases, thus generating wave images depicting the shear waves within the liver. The sequence is repeated four times, with the phase relationship (phase offset) between the vibrations and the oscillating motion-sensitizing gradients adjusted each time, leading to the production at each slice location of wave images located at four evenly spaced time points over the wave cycle. The total acquisition time for a patient is approximately two minutes (with four 16-second long breathholds with short recovery time in between).

At each slice location, wave images are processed automatically on a scanner computer using specialized software that utilizes an inversion algorithm to produce quantitative, cross-sectional maps called elastograms depicting tissue stiffness. Four elastograms, one at each of the four slice locations, are generated. The elastograms are color maps that depict stiffness in different regions of the liver with a color scale in units of kilopascals (kPa). The elastograms are transferred offline for analysis (9, 10) by a single experienced image analyst in the MR3T research laboratory with at least six months of experience working with MRE. The image analyst uses a custom software package to manually draw regions of interest (ROI) on the elastograms. ROIs are drawn at each of four slice locations in areas of the liver where the corresponding wave images depict clearly observable wave propagation, and avoiding artifacts, large blood vessels, and liver edges. The mean liver stiffness was calculated by averaging the per-pixel stiffness values across ROIs at four slice locations. The final results are automatically outputted to an electronic spreadsheet.

1. Boyd NF, Dite GS, Stone J, Gunasekara A, English DR, McCredie MR, et al. Heritability of mammographic density, a risk factor for breast cancer. The New England journal of medicine. 2002;347(12):886-94.
2. Hooker JC PC, Liao S, Le TA, Chen J, Wolfson T, Middleton MS, Loomba R, Sirlin C. Inter-reader reproducibility of MRI hepatic proton density fat fraction (PDFF) estimation in adults with biopsy-proven NASH. Abstract presentation at ESGAR, Paris, June 2015.
3. Loomba R, Wolfson T, Ang B, Hooker J, Behling C, Peterson M, et al. Magnetic resonance elastography predicts advanced fibrosis in patients with nonalcoholic fatty liver disease: a prospective study. Hepatology (Baltimore, Md). 2014;60(6):1920-8.
4. Yin M, Talwalkar JA, Glaser KJ, Manduca A, Grimm RC, Rossman PJ, et al. Assessment of hepatic fibrosis with magnetic resonance elastography. Clinical gastroenterology and hepatology : the official clinical practice journal of the American Gastroenterological Association. 2007;5(10):1207-13.e2.
5. Chen J, Talwalkar JA, Yin M, Glaser KJ, Sanderson SO, Ehman RL. Early detection of nonalcoholic steatohepatitis in patients with nonalcoholic fatty liver disease by using MR elastography. Radiology. 2011;259(3):749-56.
6. Kim D, Kim WR, Talwalkar JA, Kim HJ, Ehman RL. Advanced fibrosis in nonalcoholic fatty liver disease: noninvasive assessment with MR elastography. Radiology. 2013;268(2):411-9.
7. Venkatesh SK, Yin M, Ehman RL. Magnetic resonance elastography of liver: technique, analysis, and clinical applications. Journal of magnetic resonance imaging : JMRI. 2013;37(3):544-55.
8. Loomba R, Schork N, Chen CH, Bettencourt R, Bhatt A, Ang B, et al. Heritability of Hepatic Fibrosis and Steatosis Based on a Prospective Twin Study. Gastroenterology. 2015;149(7):1784-93.
9. Noureddin M, Lam J, Peterson MR, Middleton M, Hamilton G, Le TA, et al. Utility of magnetic resonance imaging versus histology for quantifying changes in liver fat in nonalcoholic fatty liver disease trials. Hepatology (Baltimore, Md). 2013;58(6):1930-40.
10. Permutt Z, Le TA, Peterson MR, Seki E, Brenner DA, Sirlin C, et al. Correlation between liver histology and novel magnetic resonance imaging in adult patients with non-alcoholic fatty liver disease - MRI accurately quantifies hepatic steatosis in NAFLD. Alimentary pharmacology & therapeutics. 2012;36(1):22-9.